Engineered Science
DOI: https://dx.doi.org/10.30919/es988

Boosting Microwave Absorption Performance of Bio-Gel Derived Co/C Nanocomposites

Yiming Zhong,[1, 2] Dechun Liu,[3] Qiuyun Yang,[1] Yunpeng Qu,[1,*] Changyou Yu,[2] Kelan Yan,[4,*] Peitao Xie,[2,*] Xiaosi Qi,[1] Zhanhu Guo[5] and Zhexenbek Toktarbay[6,*]

Abstract

The Co/C nanocomposites toward outstanding electromagnetic (EM) microwave absorption were meticulously designed and prepared by bio-gel method. The Co nanoparticles were embedded into the carbon network constructed by agar powder. Our obtained Co/C nanocomposites exhibited excellent EM wave absorption performance including wide bandwidth (7.1 GHz), thin thickness (1.71 mm), light weight and wide effective absorbing frequency. Dielectric relaxation at multilayer interfaces, porous biomass carbon materials and magnetic Co nanoparticles are the main sources for enhancing the wave absorption properties. The amorphous carbon in the material prevents the condensation and oxidation of magnetic Co nanoparticles, thus contributing to the generation of good impedance matching. On the basis of the percolation theory, the optimal Co content was determined, and a percolation model suitable for Co/C materials was established.

Keywords: High-performance microwave absorption; Dielectric loss; Magnetic loss; Porous Co/C nanocomposites; Percolation.
Received: 11 September 2023; Revised: 12 October 2023; Accepted: 16 October 2023.
Article type: Research article.

1. Introduction

With the development and progress of modern electronic science and technology, excessive electromagnetic (EM) wave pollution has interfered and affected people's normal production and life as well as their health.[1-4] Therefore, solving the EM wave interference problem is an inevitable and despised issue in today's society, and it is also a researching spot in EM field over the world.[5-8] Hence, new-generation absorbing materials with wide bandwidth, thin thickness, light weight and wide effective absorbing frequency are urgently needed.

In principle, when the electromagnetic wave is incident on the surface of an object medium, its direction is usually reflection, internal loss and transmission of three parts, and the electromagnetic wave can be effectively attenuated by the material is called absorbing material. Theoretically, the absorbing material consumes the electromagnetic wave by making the incident electromagnetic wave lose energy in other forms or by means of interference elimination.[5,6] The decay performance is determined by the electromagnetic properties of the material itself, namely the dielectric constant (ε', ε'') and magnetic permeability (μ', μ'').[7,8] The real part of the two parameters respectively represents the storage capacity of electric energy and magnetic energy of EM media, and the imaginary part describes the magnitude of its loss. There are usually three loss mechanisms: magnetic loss, dielectric loss and interference loss. A good absorbing material should consume as much energy as possible into the material, reducing reflection and transmission.[9,10]

At present, the development target of absorbing materials is "light, thin, wide and strong". That is, the material has the characteristics of light weight, thin thickness, wide effective absorption frequency range and large microwave absorption percentage. To meet these requirements, a lot of research and efforts have been made.[11,12] The first is "light", to meet the requirements of light, carbon materials as the main composite

[1] *College of Physics, Guizhou University, Guiyang, 550025, China.*
[2] *College of Materials Science and Engineering, Qingdao University, Qingdao, 266071, China.*
[3] *Qingdao Municipal Hospital, Qingdao, 266000, China.*
[4] *State Key Laboratory of Material-Oriented Chemical Engineering, College of Chemical Engineering, Nanjing Tech University, Nanjing, 210009, China.*
[5] *Integrated Composites Lab, Department of Mechanical and Construction Engineering, Northumbria University, Newcastle Upon Tyne, NE1 8ST, UK.*

material source of absorbing materials were mostly used.[13] Compared with ceramic materials and metal materials, the density of carbon materials is very low, so the application of carbon materials can greatly meet the target of lightweight. In addition, the lightweight can be further achieved by constructing a multistage aperture. It is well known that the hole is divided into big holes, mesoporous and microporous. The construction of multistage holes can not only further solve the problem of lightweight by reducing the density of the absorbing material, but also make the electromagnetic wave reflect several times after entering the material, thus enhancing their absorbing performance. To construct better multi-porous structure of carbon materials, biomineralization is usually used to construct biomass porous carbon materials in experiments.[14,15] The so-called biological mineralization method is an experimental method involved in imitating the formation conditions of mineralization in nature, and the microstructure of the materials with obvious bionic characteristics. As is well known, the long-term evolution of nature makes the internal structure has the congenital advantage, the biomass and the use of this method, the porous carbon, can better use of its natural biological which originally have different internal structure to make porous structure design. Therefore, in order to increase the scattering of electromagnetic waves inside the material and ultimately improve the absorption performance of the material, we meticulously designed the Co/C porous nanocomposites.[16]

Unfortunately, only the use of biomass porous carbon materials to build the absorbing material, its absorbing performance is far from meeting the demand. Pure carbon materials have only electrical responses and almost no magnetic response, which limits the improvement of their absorbing properties. But the single magnetic metal material is too heavy and chemical properties are not stable enough, easy to occur in the air oxidation and other phenomena, thereby reducing the absorption performance of the material. which affects the low weight of the material. Therefore, to optimize the wave-absorbing properties, the composite material is usually constructed with porous carbon materials and other kinds of materials, which can also reduce the weight of the material, so as to meet the need for low weight. At present, according to the different substrates and absorbents, absorbing materials can be simply categorized as the following categories: one is magnetic dielectric absorbing materials, usually functionalized by ferrite or Fe, Co, Ni and other magnetic metals; one is dielectric absorbing materials, usually using ceramic and semiconductor materials; another is a resistive absorbing material made of conductive carbon black or graphite, *etc*.[17] It was found that the absorbing materials constructed by magnetic metals, such as Fe, Co and Ni, have the advantages of high saturation magnetization, high snooker limit and strong magnetic loss, which made them excellent candidates for EM absorbing.[18-20]

Therefore, Co/C nanocomposites were meticulously designed and fabricated by bio gel-derived method in this study, so that magnetic Co nanoparticles could be evenly distributed in the carbon matrix network constructed by agar. The absorbing nanocomposites has the advantages of light weight, thin thickness, wide effective absorption frequency and large microwave absorption percentage. The filling content of Co/C in absorbing coating was optimized by percolation theory, and good impedance matching was obtained. Due to the porous structure and multilayer interface, absorbing composites have many different dielectric response regions, which is conducive to enhancing the dielectric loss capacity to achieve good electromagnetic wave absorption performance. On the other side, the high-frequency diamagnetism of the agar carbon mesh can be offset to a certain extent by the magnetism of the cobalt metal particles. High-performance absorbing materials with light weight, thin thickness and large preparation scale were prepared by bio-gels technology. As for the synthesis steps of Co/C nanocomposites in this experiment and the corresponding proportioning parameters, we have given a detailed description and flowchart explanation in the supplementary materials.

2.Results and discussions

The composition and microstructure of absorbing materials closely correlates with their electromagnetic wave absorption properties. Therefore, XRD and Raman spectroscopy are used to analyze the microstructure and composition of the materials to explain why the materials constructed in this way have excellent absorption properties. The structure information and crystallization conditions of the material are illustrated by Raman spectroscopy and XRD. XRD patterns were obtained for nanocomposites and pure carbon powders. As shown in Fig. 1a, the diffraction peaks of cubic Co were obviously observed. Pure carbon powder has a wide peak at $2\theta = 26°$, while graphite carbon has no characteristic peak at $2\theta = 44°$, manifesting that amorphous carbon is the main form of carbon in Co/C nanocomposites. The pyrolysis of agar powder produces

[6] *Laboratory* of Engineering Profile, Satbayev University, Satbayev St. 22a, Almaty 050013, Kazakhstan.

**Email*: *ypqu@gzu.edu.cn* (Y. Qu), *lyan@njtech.edu.cn* (K. Yan), *xiepeitao1991@qdu.edu.cn* (P. Xie), *zhexenbek.toktarbay@gmail.com* (Z. Toktarbay)

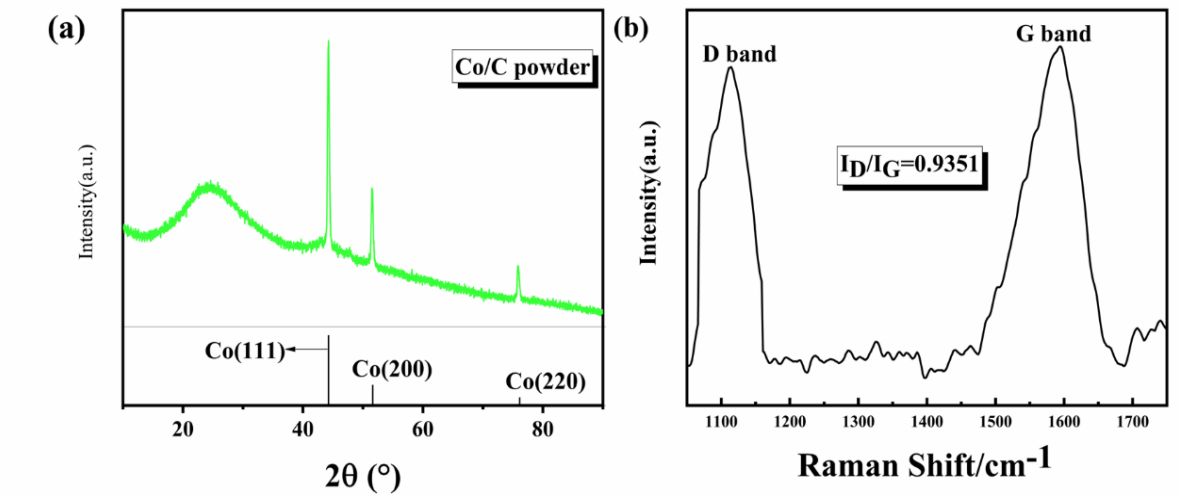

Fig. 1 XRD pattern(a) and Raman spectrum (b) of the Co/C nanocomposites (Co/C 0.15 mol/L 15%).

amorphous carbon, while cobalt is produced by the thermal decomposition reaction of $CoCO_3$ and the thermal reduction caused by carbon.

The detailed carbon composition of the Co/C nanocomposite has been studied using Raman spectroscopy. As shown in the Fig. 1b, Raman spectra show that pure toner and Co/C nanocomposites have two peaks, namely D peak at 1100 cm^{-1} and G peak at 1594 cm^{-1}. The G-band is known to be caused by in-plane vibrations of sp^2 carbon atoms; the D-band signal indicates that it is mainly amorphous carbon structure.[18-26] The higher the degree of graduation of carbon materials, the lower the I_D/I_G value. From the Fig. 2b, it can see that I_D/I_G of the Co/C nanocomposite were relatively large, which indicates that the degree of graduation of the fabricated

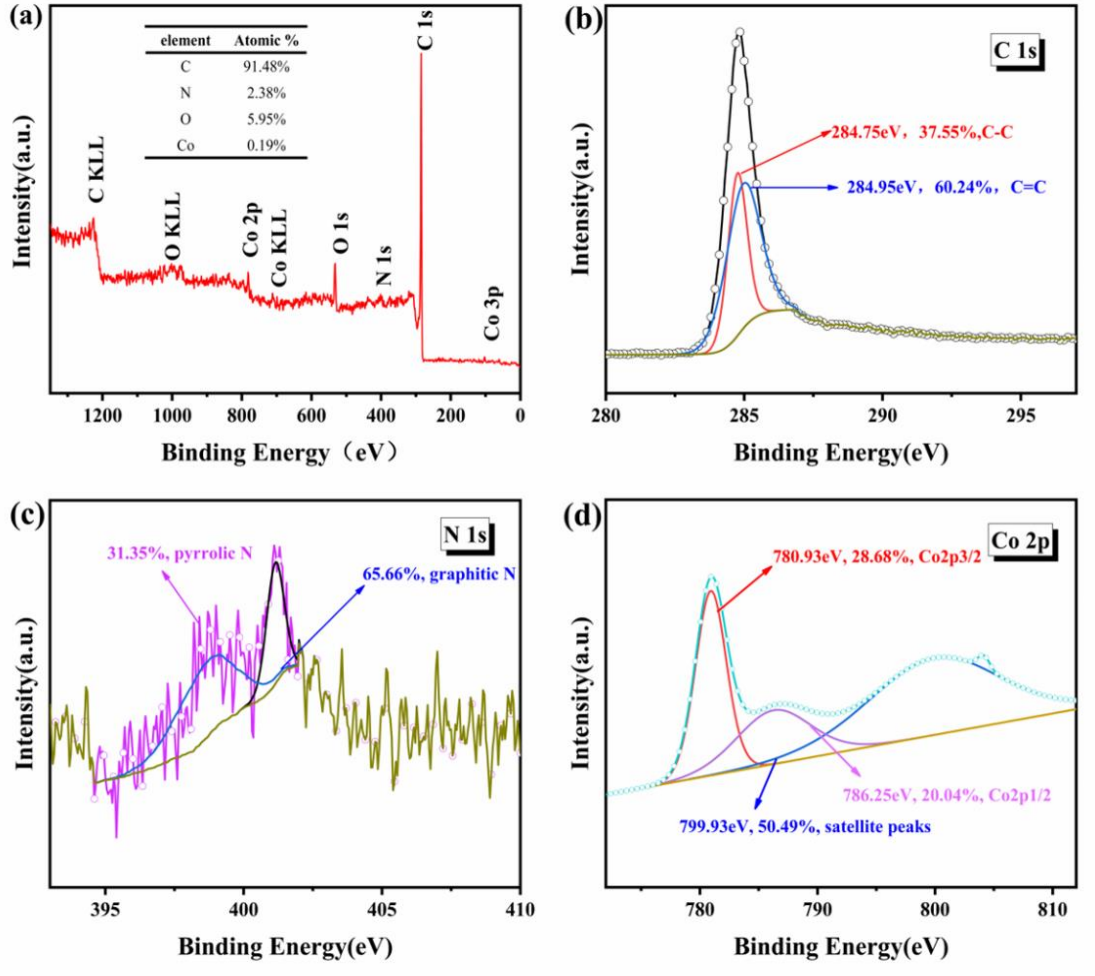

Fig. 2 XPS spectra of Co/C composites: (a) survey spectrum, (b) C 1s, (c) N 1s, and (d) Co 2p.

material is low and that the carbon inside the material is mainly crystalline carbon. The properties of crystalline carbon make it less conductive, which also favors better impedance matting. Meanwhile, it also protects the Co metal nanoparticles inside the material from oxidation, and the retention of Co metal magnetism favors the EM waves absorption due to magnetic metal particles. Moreover, the calculated I_D/I_G of the Co/C nanocomposite is 0.9351 due to the amorphous carbon, in agreement with the XRD results.[18] The XPS spectrum of the nanocomposite material is shown in Fig. 2. The presence of distinct peaks for Co, O and C in Fig. 2a indicates that the main constituent elements in the material are C, O and Co. The 1s of C are divided into three peaks, denoted C=C and C-O-C respectively.[33,34] However, we found that the two forms of carbon did not take up all the proportion, so it is inferred that there should be a small part of C-O-C, which can interact with electromagnetic to enhance the wave-absorbing performance.[35-40]

Scanning electron microscopy (SEM) was used for analyzing some detailed structural information of materials. As dipected in the Fig. 3, the SEM image presented that the material has a porous honeycomb shape with a pore diameter of about 7 μm and a thin pore wall thickness of about 500-1000 nm. From the observations in Fig. 3, it can see that the walls of these pores are littered with several tiny particles. Observations in the unfolded state show that the distribution of cobalt nanoparticles is relatively uniform at concentrations of 0.05 mol/L and 0.15 mol/L, and that there is no mass aggregation. At a concentration of 0.25 mol/L, agglomeration occurs for some particles. More SEM images can be viewed in the supplementary material.

Figure 4 provides the reflection loss (RL) curves at diverse frequencies and thicknesses. Based on the data analysis, we find that the optimal RL at each concentration is 15 % component content. When RL = -10 dB, the material is able to absorb 90% of the incident electromagnetic wave. When RL = -20 dB, 99% of the incident electromagnetic wave is absorbed.[41] However, in practice, the highest absorption strength is not necessarily the most critical issue. Therefore, in practical application, we usually regard RL < -10 dB, *i.e.*, 90% absorption, as the effective absorption of materials for electromagnetic waves. Within a certain range of frequencies and thicknesses, the four samples can effectively absorb electromagnetic waves, but different samples have different levels of effective absorption. The ratio of the Co/C content has a significant effect on the reflection loss.

The minimum RL of pure carbon sample (a) is -30.4 dB when the thickness is 2.26 mm, and the maximum RL is 4.6 GHz, when the thickness is 2.01 mm. For sample (b) of 1.71 mm, the RL_{min} is -26.5 dB, and the sample of 1.75 mm, the

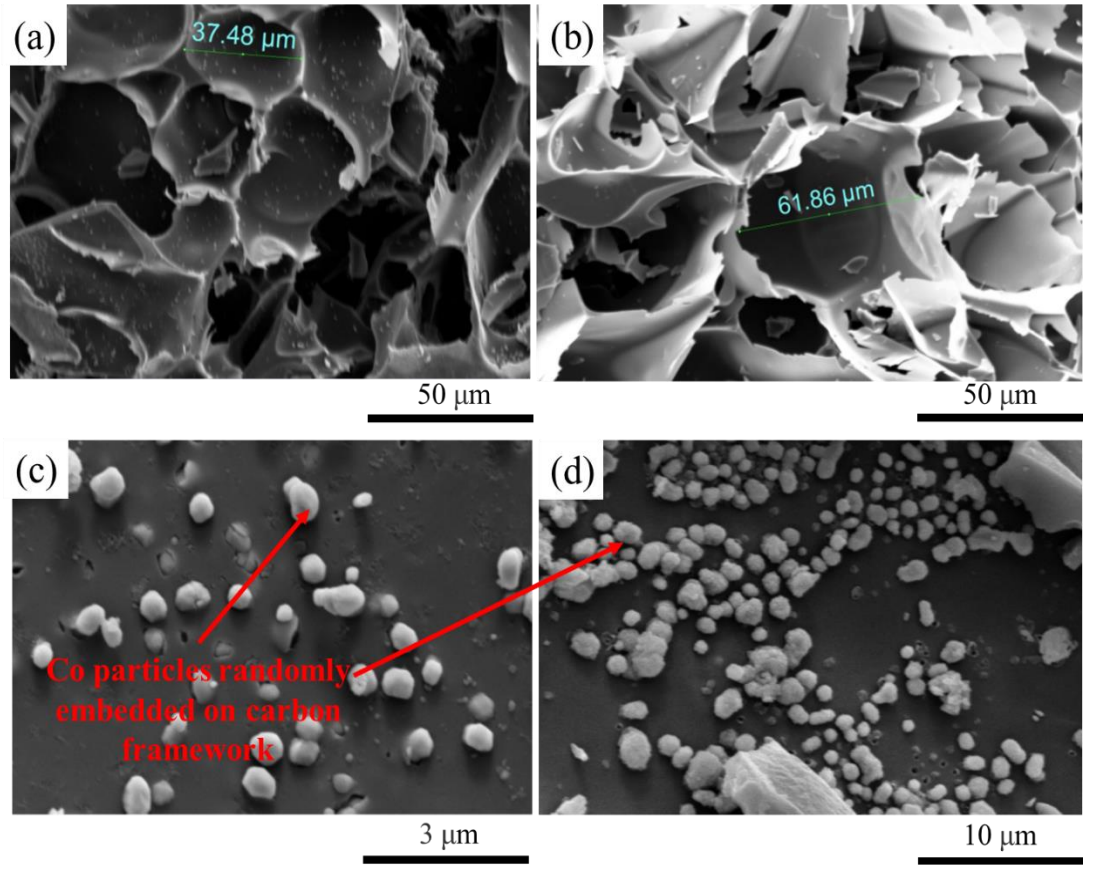

Fig. 3 SEM images of the Co/C nanocomposites.

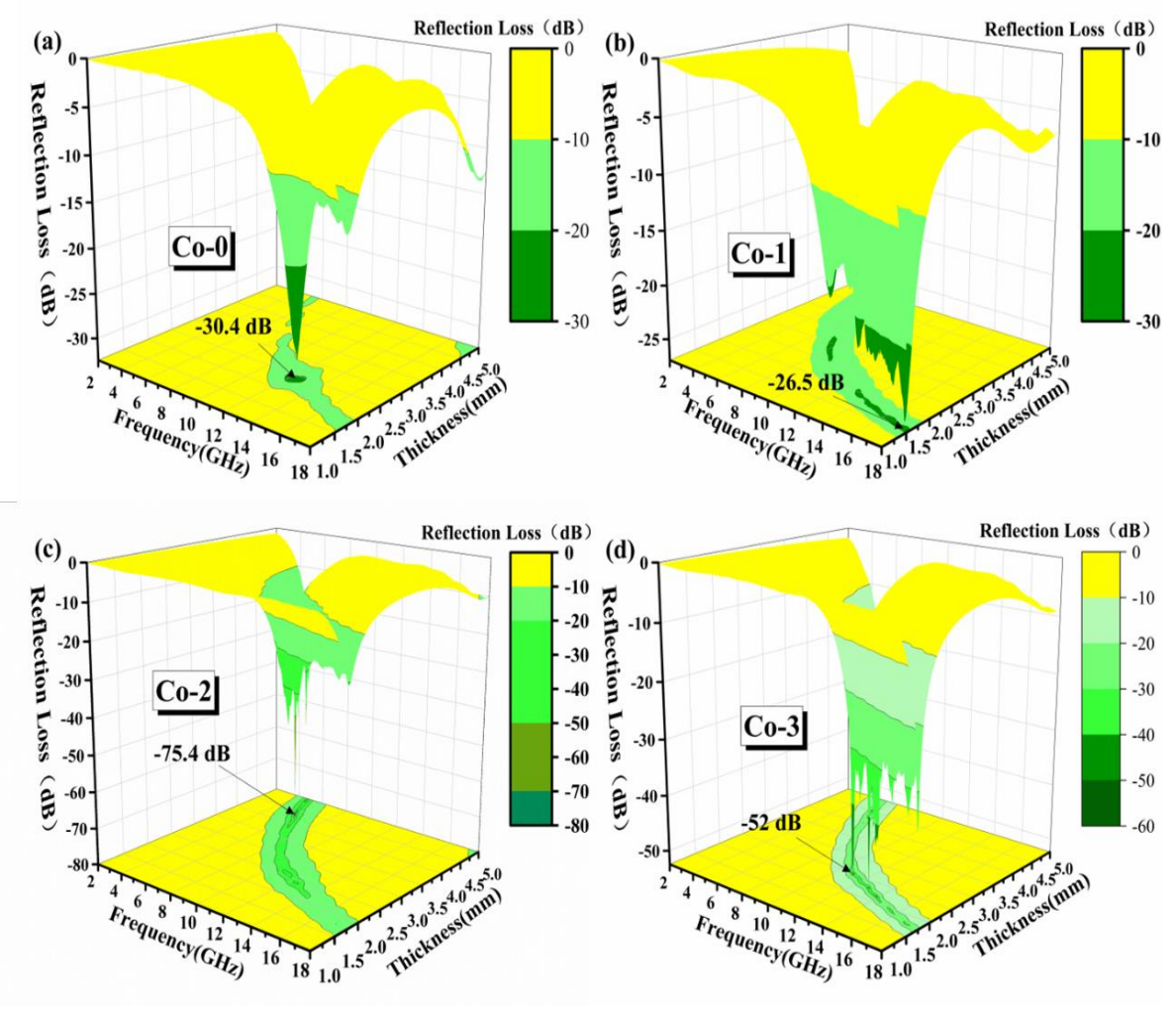

Fig. 4 Three-dimensional reflection loss curves for the paraffin composites.

maximum bandwidth is 6.9 GHz, which shows the best overall absorption performance for electromagnetic waves. The Co/C content ratio of sample (c) was 0.15 mol/L, the sample (c) has a minimum RL of -75.4 dB and a maximum broadband width of 6.4 GHz at a thickness of 1.98 mm. For sample (d) of 2.01 mm thickness, the RL_{min} value is -52 dB. When the thickness of sample (d) is 1.98 mm, its maximum broadband width is 7.1 GHz.[38] Through the experimental data, it is not difficult to see that compared with EM wave absorption capacity of pure carbon sample, that of sample (b) and sample (c) increases with the increase of Co/C content ratio, and the absorption performance of sample (c) is better than that of sample (b), while the electromagnetic wave absorption performance of sample (d) is relatively worse than that of sample (c). Therefore, we can know that the addition of magnetic cobalt nanoparticles can enhance the absorption performance of carbon materials, and the increase of the number of magnetic cobalt nanoparticles in a certain range can improve the EM wave absorption performance, but too much amount will also have a negative impact on the absorption performance of carbon materials.

To assess the absorption capacity, the absorption performance of Co/C nanocomposites from this work and other works are listed in Table 1. Compared to other Co/C nanocomposites, the nanocomposite fabricated in this work has a thinner thickness, a wider bandwidth and a stronger absorption capacity of electromagnetic waves, which demonstrates that the nanocomposite fabricated in this study has good electromagnetic wave absorption property. As everyone knowns that outstanding absorption function means that EM waves can easily enter into the EM medium and lost as much as possible inside the material, and impedance matching parameter is the key factor to evaluate this behavior. The impedance ratio $Z_{in}/Z_0 = 1$ indicates that EM waves can perfectly entry into EM medium, which is hardly obtained in real materials, but the closer Z_{in}/Z_0 is to 1, the better the impedance match of electromagnetic wave-absorbing materials. In this paper, $Z_{in}/Z_0 = 0.8\text{-}1.2$ is used to estimate the impedance matting of the fabricated nanocomposites.

Table 1. EM wave absorption properties of the previously reported Co nanomaterials and this work.

Materials	Content-mass ratio (%)	RL_{min}	Matching Thickness (mm)	Frequency range (GHz)	d(RL<-10dB)	Ref.
Co/C	30	-52.42 dB	1.93 mm	2.9 GHz	2.00mm	[27]
Co/C	50	-56.9 dB	1.92 mm	2.7 GHz	2.00mm	[28]
Co/C	30	-18.0 dB	3.20 mm	3.6 GHz	2.00mm	[29]
CoNi/C	35	-46.0dB	2.00 mm	5.5 GHz	2.00mm	[30]
Co/C	20	-56.0 dB	3.50mm	3.6GHz	2.30mm	[31]
Co/CNTs	20	-36.5dB	4.10mm	2.9GHZ	1.80mm	[32]
Co/C	17.5	-75.4 dB	3.85 mm	6.4 GHz	1.98mm	This work
Co/C	15	-26.5 dB	1.71mm	6.9 GHz	1.75mm	This work

The impedance ratio Z_{in}/Z_0 can be expressed as:[41-45]

$$Z_{in}=Z_0(\mu_r/\varepsilon_r)^{1/2}\, tanh\left\{j\left(2\pi f\frac{d}{c}\right)(\mu_r/\varepsilon_r)^{1/2}\right\} \quad (1)$$

$$RL(dB)=20\lg\left|\frac{(Z_{in}-Z_0)}{(Z_{in}+Z_0)}\right| \quad (2)$$

where j means the unreliable number, f is the frequency of EM wave, d is the thickness of paraffin composite, and c is the light velocity in vacuum.

Z_{in}/Z_0 is calculated by formula (1). From the figure, it can see the three-dimensional (3D) impedance ratios of the four samples have different thicknesses and frequencies. By comparing Figs. 5a, b and c, it is not difficult to see that the effective impedance matching range first increases and then decreases as the Co/C content ratio increases, even up to a certain content, but there is almost no effective impedance matching range. Therefore, we can conclude that the optimal impedance matching could be attained at the certain range of Co/C content ratios. We analyzed its relationship between material impedance matching and Co content by studying impedance matching images with different Co/C content ratios at 0.15 mol/L concentration. In the experiment, images with Co volume fraction content of 10%, 15%, 17.5% and 20% were selected and named as specimen a, b, c and d respectively. Through the analysis of sample (a) and sample (b) images, the incremental Co/C content ratio and impedance matching performance of 15 % content is significantly more excellent

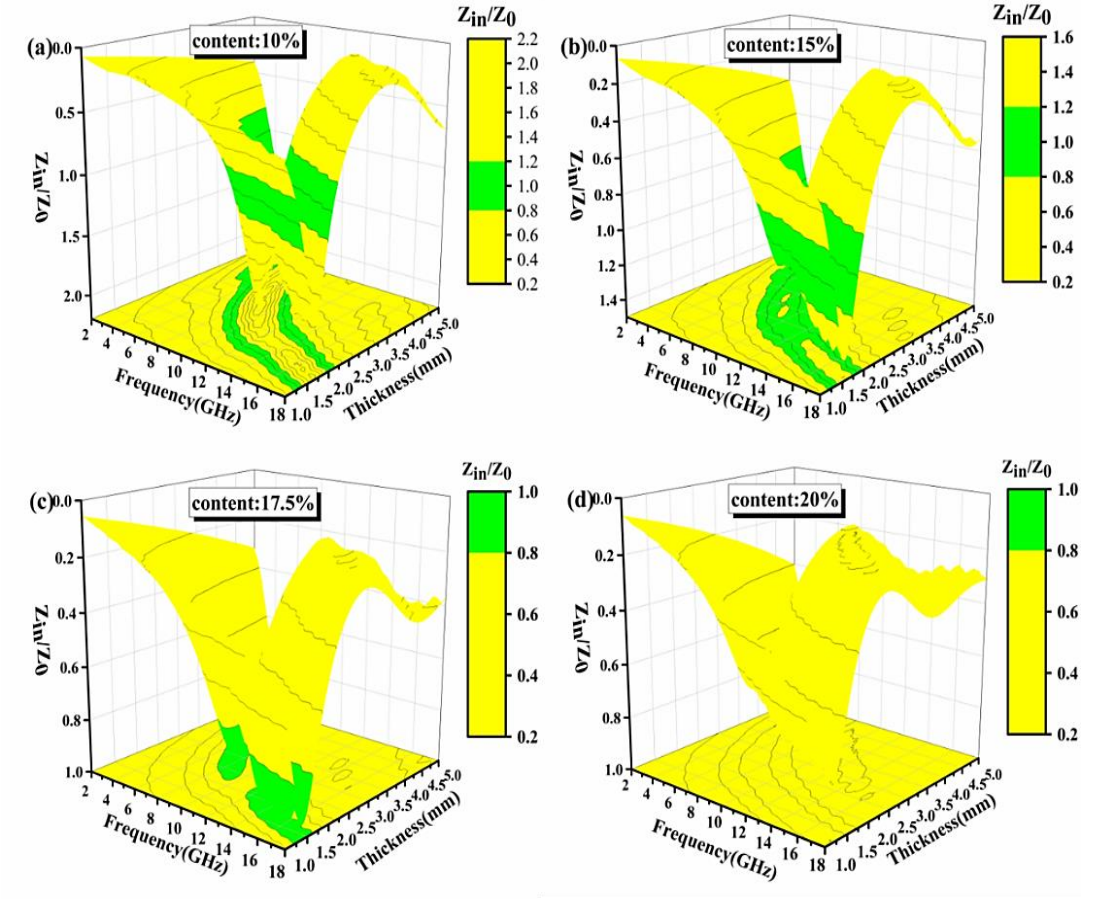

Fig. 5 The three-dimensional impedance ratio of Co/C nanomaterials at different contents.

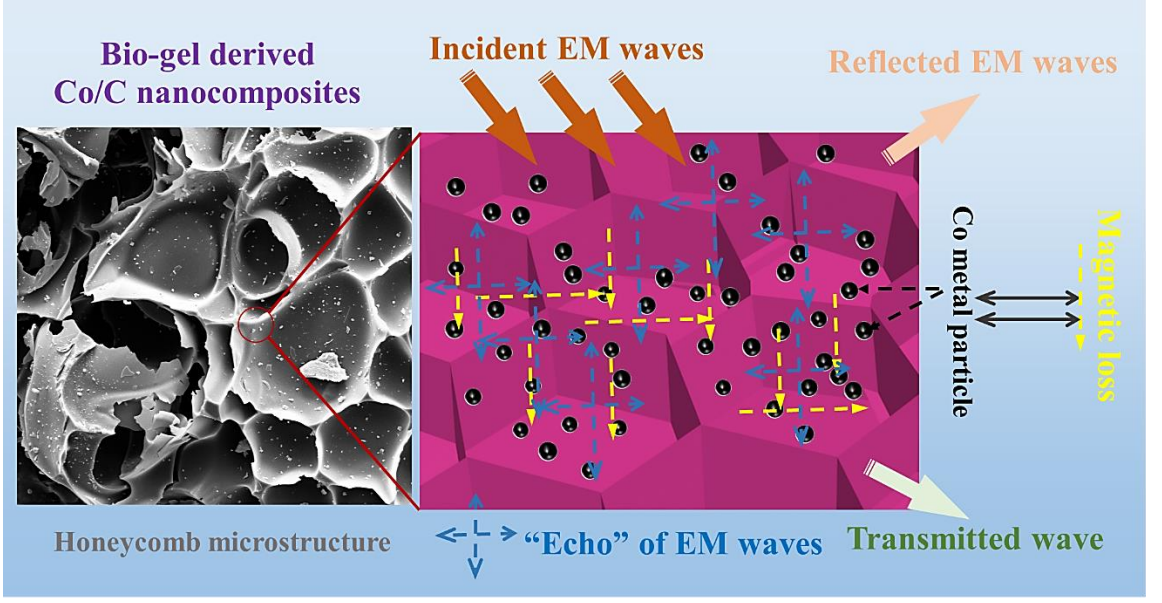

Fig. 6 Schematic for EM microwave absorption mechanism.

than that of 10 % content, which proves that the addition of metal Co improves the impedance matching function of materials.

Figure 6 shows the wave absorbing mechanism of Co/C nanocomposites. Through SEM images, we can see that the material almost presents a honeycomb-like structure. When electromagnetic waves are injected into the material, the internal honeycomb-like structure can make electromagnetic waves reflect inside for many times, thus attenuating electromagnetic waves. Similarly, the magnetic loss caused by the Co metal particles in the material will also attenuate electromagnetic waves, thereby improving the wave absorption performance.

Figures 5c-d show that as the Co/C ratio increases, the impedance matching becomes worse while its effective impedance matching region becomes smaller. The effective impedance matching in Fig. 5c is split into two parts, while in d there is almost no effective impedance matching. It is also shown that when the Co/C content ratio reaches a certain value, the impedance matching of the material becomes worse with increasing content, leading to a deterioration of its absorption performance. This also explains why the absorption performance deteriorates when the ratio of Co/C content in the RL map is too large. However, when the ratio of Co/C content is too large, the decay competence of the sample is sufficient to absorb and attenuate electromagnetic waves. However, due to the poor impedance matching of the material, as shown in the figure for 20 % proportion content, when the content is too large, it is almost not in the range of Z_{in}/Z_0 =0.8 to 1.2, resulting in the overall electromagnetic wave absorption performance of the material.[39,40] Therefore, it was need to find the optimal ratio of Co/C content through experimental data to achieve the best match of material impedance matching and attenuation capability for the best absorption performance.

In fact, a good performance of absorbing material not only needs good impedance matching, also needs to have excellent attenuation competence to burn off the incoming electromagnetic wave, because good impedance matching only said material is able to allow the electromagnetic wave into attenuation factor (α) calculated by the formula (3), diagram for the four samples of the relationship between frequency and attenuation factor. The attenuation coefficient of the pure carbon sample is inferior to that of the 0.05 mol/L sample, and its absorption is stronger. The reason for this is that 0.05 mol/L not only has a better impedance matching than the pure carbon sample, but also a better attenuation factor, which is consistent with the fact that the attenuation factor and impedance matching jointly determine the absorption capacity. However, the decay factors of 0.15-0.25 mol/L are worse than those of 0.05 mol/L, which leads to a reduction in the attenuation and loss capacity of the material to electromagnetic waves. As shown in Fig. 7**,** the adsorption properties of 0.15 mol/L and 0.25 mol/L are better than those of pure carbon. From this, it can be concluded that the higher the impedance matching is not the better, because when the high impedance matching, the attenuation factor is reduced, resulting in the electromagnetic wave cannot enter into the materials well, thereby reducing the absorption performance. However, if the attenuation factor is too low, the incident electromagnetic wave will be less lost, and the absorption performance of the materials will be reduced. Therefore, we need to choose the appropriate size of the attenuation factor

and find a suitable impedance matching and attenuation factor coordination range. The α can be expressed as:[46-50]

$$\alpha = \frac{\sqrt{2}\pi f}{c} \times \sqrt{(\mu''\varepsilon'' - \mu'\varepsilon') + \sqrt{(\mu''\varepsilon'' - \mu'\varepsilon')^2 + (\mu'\varepsilon'' + \mu''\varepsilon')^2}} \quad (3)$$

where μ' and μ'' are complex permeability, ε' and ε'' are complex permittivity.

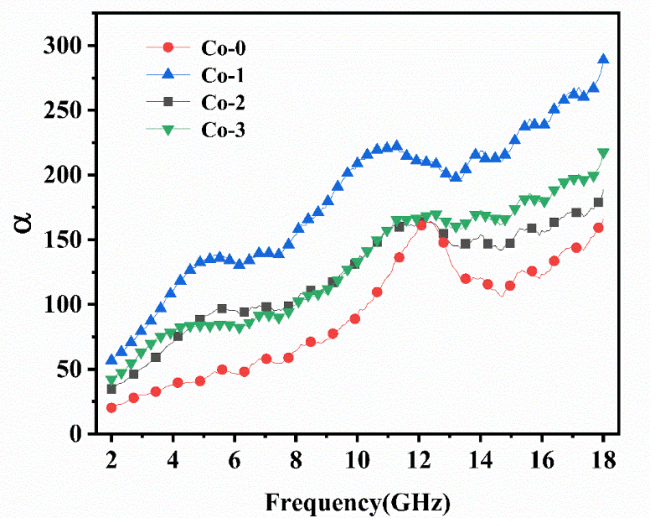

Fig. 7 Frequency dependances of the attenuation factor (α) for four samples.

The complex ε and μ are two fundamental electromagnetic parameters that affect the interaction of an absorbing material with electromagnetic waves. The electromagnetic parameters of the material were studied and its effect of Co/C ratio on absorption properties of material was determined and demonstrated. Fig. 8 shows that ε' decreases with increasing Co/C ratio at 12.5 % and 15 % content (volume fraction), which is actually different from the normal perception. Since in the testing process we usually use paraffin and samples to construct the composite material, since their quality is determined, an increase in the Co/C ratio will increase the mass of the powder and thus decrease the volume fraction of the paraffin composite sample. The higher the concentration of the Co element, the smaller the volume fraction of the paraffin complex, so a decrease in the sample volume fraction generally leads to a decrease in the permittivity. In the range of 11 GHz to 15 GHz, there is a clear virtual peak and a significant reduce in the real component of the permittivity due to dielectric relaxation phenomena.[51-55]

Figure 9a shows the tangent diagram of the dielectric loss of the prepared Co/C nanocomposite. There is a strong peak near 15 GHz, indicating that there is a strong dielectric loss here, which can correspond to a strong electromagnetic absorption band.

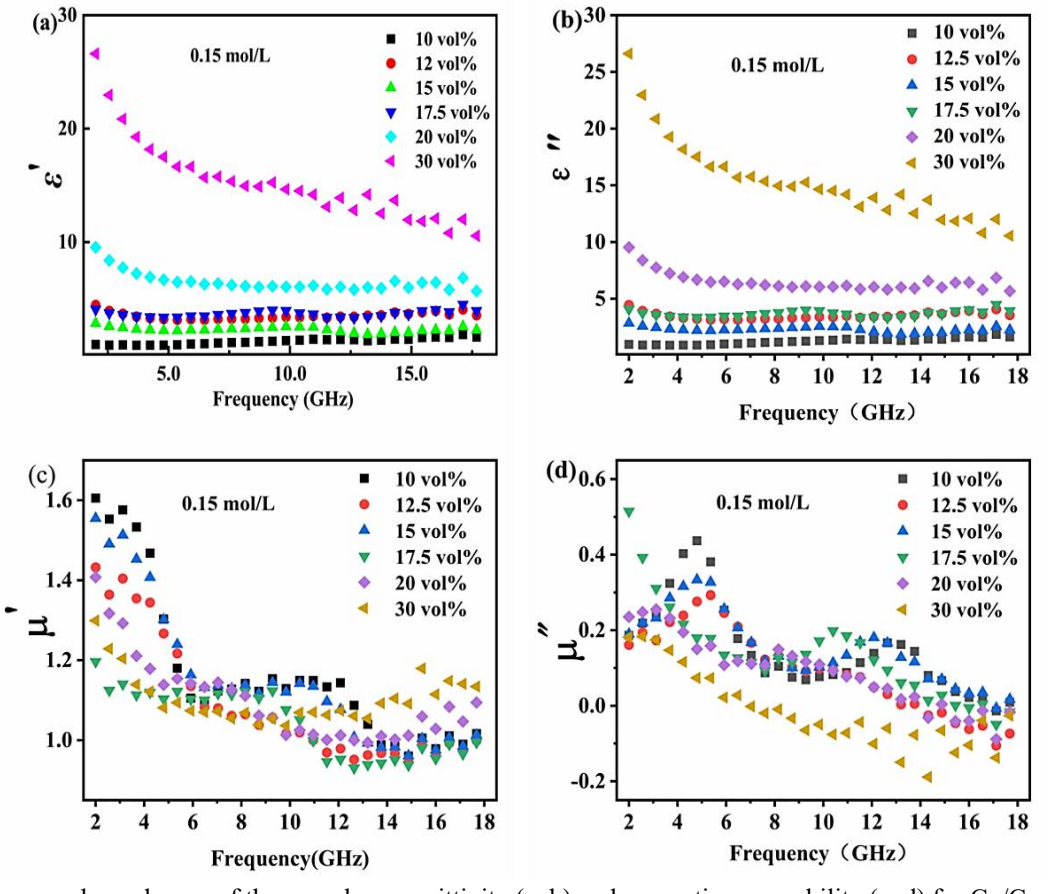

Fig. 8 Frequency dependences of the complex permittivity (a, b) and magnetic permeability (c, d) for Co/C composites.

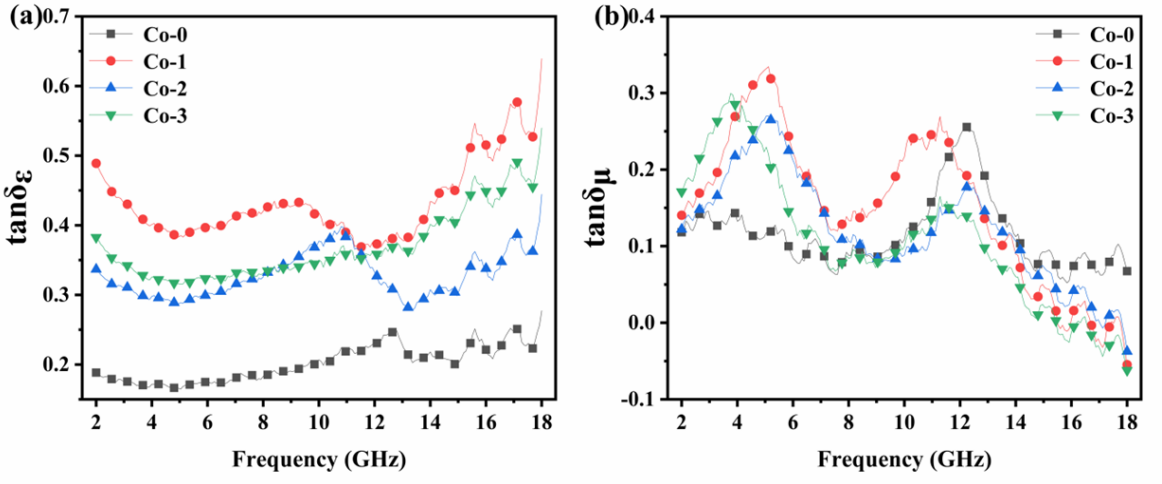

Fig. 9 Image of dielectric loss tangent (a) and magnetic loss tangent (b) for the nanocomposites.

According to the combination of Fig. 8 and Fig. 9, there are obvious loss peaks in the dielectric loss and magnetic loss curves of 12 ~ 18 GHz, and the Co-1 sample has the best comprehensive loss performance. Although Co-0, the blank group, has excellent magnetic loss performance, its dielectric loss is very poor, so its comprehensive absorption performance is the worst.

The C_0 is always used to express the contribution of eddy current loss to magnetic loss and is expressed by the formula (4):[56-60]

$$C_0 = \mu"/(\mu'^2 f) \quad (4)$$

$$\mu" = 2\pi\mu_0(\mu'^2)\sigma d^2 f/3 \quad (5)$$

As can be seen in Fig. 10, the value of C_0 changes significantly with increasing frequency and shows decreasing trend, indicating that vortex loss is absent in the nanocomposite. Therefore, the magnetic losses of the composite are dominated by natural resonance losses, and the representative hysteresis losses are also too feeble in the GHz frequency scope.[43-46] The absorption capacity of electromagnetic waves is a result of the combination of dielectric and magnetic losses. The experimental results show that the effect of dielectric loss on the absorbing properties of materials is dominant in this experiment. Therefore, when the peaks of ε'' and μ'' are inconsistent, the influence of ε'' on absorption capacity should be paid more attention.[56-62]

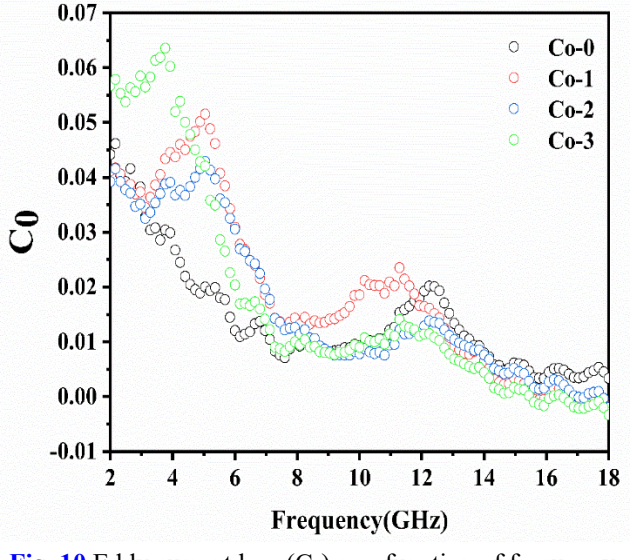

Fig. 10 Eddy current loss (C_0) as a function of frequency.

4. Conclusion

Here, the bio-gel based technology to fabricate a new porous Co/C nanocomposite was proposed. The amorphous carbon holds back the aggregation of Co nanoparticles, resulting in excellent impedance matching. On the basis of the seepage doctrine, the optimal ratio of Co/C content in the composite material was determined to make it have a good impedance matching. Under the condition of thin thickness, light weight and wide band, excellent reflection loss (RL < -10 dB) was obtained. Its excellent absorption performance originated from the resonances of cobalt nanoparticles in multilayer carbon structure and dielectric relaxation losses. This research offers a brand-new paradigm for confirming the optimal absorbent content by percolation theory which will trigger greatly real-world applications on EM fields.

Acknowledgement

This work was supported by the National Natural Science Foundation of China [52101176], Natural Science Foundation of Shandong Province (ZR2020QE006). The author (Yunpeng Qu) also acknowledges the Fund of Natural Science Special (Special Post) Research Foundation of Guizhou University [Grant No. 2023-032].

Conflict of Interest

There is no conflict of interest.

Supporting Information

Applicable.

References

[1] F. Shahzad, M. Alhabeb, C. B. Hatter, B. Anasori, S. Man Hong, C. M. Koo, Y. Gogotsi, Electromagnetic interference shielding with 2D transition metal carbides (MXenes), *Science*, 2016, **353**, 1137-1140, doi: 10.1126/science.aag2421.

[2] T. J. Cui, S. Liu, G. D. Bai, Q. Ma, Direct transmission of digital message via programmable coding metasurface, *Research*, 2019, **2019**, 1-12, doi: 10.1155/2019/2584509.

[3] W. Fan, J. Yin, C. Yi, Y. Xia, Z. Nie, K. Sui, Nature-inspired sequential shape transformation of energy-patterned hydrogel sheets, *ACS Applied Materials & Interfaces*, 2020, **12**, 4878-4886, doi: 10.1021/acsami.9b19342.

[4] D. Zhang, H. Qiao, W. Fan, K. Zhang, Y. Xia, K. Sui, Self-powered ionic sensors overcoming the limitation of ionic conductors as wearable sensing devices, *Materials Today Physics*, 2020, **15**, 100246, doi: 10.1016/j.mtphys.2020.100246.

[5] L. Chen, S. Mao, P. Wang, Z. Yao, Z. Du, Z. Zhu, L. A. Belfiore, J. Tang, Visible light driven hot-electron injection by Pd nanoparticles: fast response in metal-semiconductor photodetection, *Advanced Optical Materials*, 2021, **9**, 2001505, doi: 10.1002/adom.202001505.

[6] H. Zhang, Z. Jia, B. Wang, X. Wu, T. Sun, X. Liu, L. Bi, G. Wu, Construction of remarkable electromagnetic wave absorber from heterogeneous structure of Co-$CoFe_2O_4$@mesoporous hollow carbon spheres, *Chemical Engineering Journal*, 2021, **421**, 129960, doi: 10.1016/j.cej.2021.129960.

[7] D. Lan, M. Qin, J. Liu, G. Wu, Y. Zhang, H. Wu, Novel binary cobalt nickel oxide hollowed-out spheres for electromagnetic absorption applications, *Chemical Engineering Journal*, 2020, **382**, 122797, doi: 10.1016/j.cej.2019.122797.

[8] Yurun, Feng, Enhanced electromagnetic microwave absorption of Fe/C/SiCN composite ceramics targeting in integrated structure and function, *Ceramics International*, 2021, **47**, 3842-3852, doi: 10.1016/j.ceramint.2020.09.244.

[9] P. Xie, Y. Liu, M. Feng, M. Niu, C. Liu, N. Wu, K. Sui, R. R. Patil, D. Pan, Z. Guo, R. Fan, Hierarchically porous Co/C nanocomposites for ultralight high-performance microwave absorption, *Advanced Composites and Hybrid Materials*, 2021, **4**, 173-185, doi: 10.1007/s42114-020-00202-z.

[10] B. Quan, W. Shi, S. J. H. Ong, X. Lu, P. L. Wang, G. Ji, Y. Guo, L. Zheng, Z. J. Xu, Defect engineering in two common types of dielectric materials for electromagnetic absorption applications, *Advanced Functional Materials*, 2019, **29**, 1901236, doi: 10.1002/adfm.201901236.

[11] Z. Jia, B. Wang, A. Feng, J. Liu, M. Zhang, Z. Huang, G. Wu, Development of spindle-cone shaped of Fe/α-Fe_2O_3 hybrids and their superior wideband electromagnetic absorption performance, *Journal of Alloys and Compounds*, 2019, **799**, 216-223, doi: 10.1016/j.jallcom.2019.05.336.

[12] Y. Hao, Z. Leng, C. Yu, P. Xie, S. Meng, L. Zhou, Y. Li, G. Liang, X. Li, C. Liu, Ultra-lightweight hollow bowl-like carbon as microwave absorber owning broad band and low filler loading, *Carbon*, 2023, **212**, 118156, doi: 10.1016/j.carbon.2023.118156.

[13] G. Fan, Y. Jiang, J. Xin, Z. Zhang, X. Fu, P. Xie, C. Cheng, Y. Liu, Y. Qu, K. Sun, R. Fan, Facile synthesis of Fe@Fe_3C/C nanocomposites derived from bulrush for excellent electromagnetic wave-absorbing properties, *ACS Sustainable Chemistry & Engineering*, 2019, **7**, 18765-18774, doi: 10.1021/acssuschemeng.9b02913.

[14] G. Fan, Y. Jiang, C. Hou, X. Deng, Z. Liu, L. Zhang, Z. Zhang, R. Fan, Extremely facile and green synthesis of magnetic carbon composites drawn from natural bulrush for electromagnetic wave absorbing, *Journal of Alloys and Compounds*, 2020, **835**, 155345, doi: 10.1016/j.jallcom.2020.155345.

[15] P. Xie, W. Sun, A. Du, Q. Hou, G. Wu, R. Fan, Epsilon-negative carbon aerogels with state transition from dielectric to degenerate semiconductor, *Advanced Electronic Materials*, 2021, **7**, 2000877, doi: 10.1002/aelm.202000877.

[16] R. Chandra, B. Shivamurthy, S. Gowda, M. Kumar, Flexible Linear Low-density Polyethylene Laminated Aluminum and Nickel Foil Composite Tapes for Electromagnetic Interference Shielding, *Engineered Science*, 2023, **21**, 777, doi: 10.30919/es8d777

[17] J. Qiao, X. Zhang, D. Xu, L. Kong, L. Lv, F. Yang, F. Wang, W. Liu, J. Liu, Design and synthesis of TiO_2/Co/carbon nanofibers with tunable and efficient electromagnetic absorption, *Chemical Engineering Journal*, 2020, **380**, 122591, doi: 10.1016/j.cej.2019.122591.

[18] P. Xie, H. Li, B. He, F. Dang, J. Lin, R. Fan, C. Hou, H. Liu, J. Zhang, Y. Ma, Z. Guo, Bio-gel derived nickel/carbon nanocomposites with enhanced microwave absorption, *Journal of Materials Chemistry C*, 2018, **6**, 8812-8822, doi: 10.1039/c8tc02127a.

[19] Z. Wang, X. Li, L. Wang, Y. Li, J. Qin, P. Xie, Y. Qu, K. Sun, R. Fan, Flexible multi-walled carbon nanotubes/polydimethylsiloxane membranous composites toward high-permittivity performance, *Advanced Composites and Hybrid Materials*, 2020, **3**, 1-7, doi: 10.1007/s42114-020-00144-6.

[20] F. Saba, S. A. Sajjadi, S. Heydari, M. Haddad-Sabzevar, J. Salehi, H. Babayi, A novel approach to the uniformly distributed carbon nanotubes with intact structure in aluminum matrix composite, *Advanced Composites and Hybrid Materials*, 2019, **2**, 540-548, doi: 10.1007/s42114-019-00115-6.

[21] Y. Zhao, X. Yang, L. Yan, Y. Bai, S. Li, P. Sorokin, L. Shao, Biomimetic nanoparticle-engineered superwettable membranes for efficient oil/water separation, *Journal of Membrane Science*, 2021, **618**, 118525, doi: 10.1016/j.memsci.2020.118525.

[22] Tianming, Jia, Constructing mixed-dimensional lightweight flexible carbon foam/carbon nanotubes-based heterostructures: an effective strategy to achieve tunable and boosted microwave absorption, *Carbon*, 2023, **206**, 364-374, doi: 10.1016/j.carbon.2023.02.046.

[23] Q. Liang, J. Zhang, X. Qi, L. Wang, J. Ding, X. Gong, J. Yang, Y. Chen, Y. Qu, Q. Peng, W. Zhong, From core@shell ZnSe/FeSe2@$MoSe_2$ to core@shell@shell magnetic

$ZnFe_2O_4$@C@$MoSe_2$ flower-like nanocomposites: an effective strategy to boost microwave absorption performance of $MoSe_2$-based nanocomposites, *Materials Today Physics*, 2023, **30**, 100952, doi: 10.1016/j.mtphys.2022.100952.
[24] W. Shao, D. Liu, T. Cao, H. Cheng, J. Kuang, Y. Deng, W. Xie, Study on favorable comprehensive properties of superhydrophobic coating fabricated by polytetrafluoroethylene doped with graphene, *Advanced Composites and Hybrid Materials*, 2021, **4**, 521-533, doi: 10.1007/s42114-021-00243-y.
[25] P. R. Saffari, S. Sirimontree, C. Thongchom, T. Jearsiripongkul, P. R. Saffari, S. Keawsawasvong, S. Kongwat, Free and forced vibration of sandwich FGM porous variable thickness nanoplates integrated with magneto-electro-elastic layers via nonlocal strain gradient theory, *Engineered Science*, 2023, 24, 918, doi: 10.30919/es918.
[26] L. Yang, X. Huang, H. Wu, Y. Liang, M. Ye, W. Lu, F. Li, T. Xu, H. Wang, Silver nanowires: from synthesis, growth mechanism, device fabrications to prospective engineered applications, *Engineered Science*, 2023, 23, 808, doi: 10.30919/es8d808.
[27] G. Fan, Y. Jiang, C. Hou, X. Deng, Z. Liu, L. Zhang, Z. Zhang, R. Fan, Extremely facile and green synthesis of magnetic carbon composites drawn from natural bulrush for electromagnetic wave absorbing, *Journal of Alloys and Compounds*, 2020, **835**, 155345, doi: 10.1016/j.jallcom.2020.155345.
[28] H. Wu, Y. Zhong, Y. Tang, Y. Huang, G. Liu, W. Sun, P. Xie, D. Pan, C. Liu, Z. Guo, Precise regulation of weakly negative permittivity in $CaCu_3Ti_4O_{12}$ metacomposites by synergistic effects of carbon nanotubes and grapheme, *Advanced Composites and Hybrid Materials*, 2022, **5**, 419-430, doi: 10.1007/s42114-021-00378-y.
[29] G. Qi, Y. Liu, L. Chen, P. Xie, D. Pan, Z. Shi, B. Quan, Y. Zhong, C. Liu, R. Fan, Z. Guo, Lightweight Fe_3C@Fe/C nanocomposites derived from wasted cornstalks with high-efficiency microwave absorption and ultrathin thickness, *Advanced Composites and Hybrid Materials*, 2021, **4**, 1226-1238, doi: 10.1007/s42114-021-00368-0.
[30] J. Yan, Y. Huang, C. Chen, X. Liu, H. Liu, The 3D CoNi alloy particles embedded in N-doped porous carbon foams for high-performance microwave absorbers, *Carbon*, 2019, **152**, 545-555, doi: 10.1016/j.carbon.2019.06.064.
[31] H. Xu, X. Yin, X. Fan, Z. Tang, Z. Hou, M. Li, X. Li, L. Zhang, L. Cheng, Constructing a tunable heterogeneous interface in bimetallic metal-organic frameworks derived porous carbon for excellent microwave absorption performance, *Carbon*, 2019, **148**, 421-429, doi: 10.1016/j.carbon.2019.03.091.
[32] Y. Huang, X. Li, X. Xu, F. Wei, Y. Wang, M. Ma, Y. Wang, D. Sun, Green and up-scalable fabrication of superior anodes for lithium storage based on biomass bacterial cellulose, *Advanced Powder Technology*, 2021, **32**, 2484-2492, doi: 10.1016/j.apt.2021.05.013.
[33] C. Ding, L. Huang, J. Lan, Y. Yu, W.-H. Zhong, X. Yang, Superresilient hard carbon nanofabrics for sodium-ion batteries, *Small*, 2020, **16**, 1906883, doi: 10.1002/smll.201906883.
[34] C. Ding, L. Huang, X. Yan, F. Dunne, S. Hong, J. Lan, Y. Yu, W.-H. Zhong, X. Yang, Robust, superelastic hard carbon with *in situ* ultrafine crystals, *Advanced Functional Materials*, 2020, **30**, 1907486, doi: 10.1002/adfm.201907486.
[35] Peifeng, Feng, Establishment of multistage gradient modulus intermediate layer between fiber and matrix via designing double "rigid-flexible" structure to improve interfacial and mechanical properties of carbon fiber/resin composites, *Composites Science and Technology*, 2020, **200**, 108336, doi: 10.1016/j.compscitech.2020.108336.
[36] M. Wang, L. Ma, L. Shi, P. Feng, X. Wang, Y. Zhu, G. Wu, G. Song, Chemical grafting of nano-SiO_2 onto graphene oxide via thiol-ene click chemistry and its effect on the interfacial and mechanical properties of GO/epoxy composites, *Composites Science and Technology*, 2019, **182**, 107751, doi: 10.1016/j.compscitech.2019.107751.
[37] Daitao, Kuang, Large-scale synthesis and outstanding microwave absorption properties of carbon nanotubes coated by extremely small FeCo-C core-shell nanoparticles, *Carbon*, 2019, **153**, 52-61, doi: 10.1016/j.carbon.2019.06.105.
[38] P. Xie, Z. Zhang, Z. Wang, K. Sun, R. Fan, Targeted double negative properties in silver/silica random metamaterials by precise control of microstructures, *Research*, 2019, **2019**, 1-11, doi: 10.1155/2019/1021368.
[39] C. Huang, X.-L. Zhang, J. Tang, D. Li, Q.-D. Ruan, L.-L. Liu, F.-Y. Xiong, B. Wang, Y. Xu, S.-H. Cui, Y. Luo, Q.-W. Li, P. K. Chu, Spatially strain-induced and selective preparation of Mo_xN (x = 1, 2) as a highly effective nanoarchitectonic catalyst for hydrogen evolution reaction in a wide pH range, *Rare Metals*, 2023, **42**, 1446-1452, doi: 10.1007/s12598-022-02227-3.
[40] L.-R. Zou, D.-D. Sang, Y. Yao, X.-T. Wang, Y.-Y. Zheng, N.-Z. Wang, C. Wang, Q.-L. Wang, Research progress of optoelectronic devices based on two-dimensional MoS_2 materials, *Rare Metals*, 2023, **42**, 17-38, doi: 10.1007/s12598-022-02113-y.
[41] J. Yang, X. Zhu, H. Wang, X. Wang, C. Hao, R. Fan, D. Dastan, Z. Shi, Achieving excellent dielectric performance in polymer composites with ultralow filler loadings via constructing hollow-structured filler frameworks, *Composites Part A: Applied Science and Manufacturing*, 2020, **131**, 105814, doi: 10.1016/j.compositesa.2020.105814.
[42] L. Sun, Z. Shi, H. Wang, K. Zhang, D. Dastan, K. Sun, R. Fan, Ultrahigh discharge efficiency and improved energy density in rationally designed bilayer polyetherimide-$BaTiO_3$/P(VDF-HFP) composites, *Journal of Materials Chemistry A*, 2020, **8**, 5750-5757, doi: 10.1039/d0ta00903b.
[43] X. Tang, Z. Zhang, D. J. P. Kumar, Y. Qu, P. Xie, G. Liang, J. Wang, Q. Yang, Q. Yang, X. Qi, Z. Guo, Flexible carbon nanotubes/polystyrene membranous composites toward ultraweakly and frequency-stable negative permittivity at kHz region, *Engineered Science*, 2023, 24, 920, doi: 10.30919/es920.
[44] C. Deng, Y. Li, H. Wang, Y. Qu, X. Qi, Z. Peng, Z. Chen, H. Shen, K. Sun, R. Fan, Spark plasma sintered graphene/copper calcium titanate ceramic composites with negative permittivity and enhanced thermal conductivity, *Ceramics International*, 2023, **49**, 16149-16155, doi: 10.1016/j.ceramint.2023.01.212.

[45] Y. Zhou, Y. Qu, L. Yin, W. Cheng, Y. Huang, R. Fan, Coassembly of elastomeric microfibers and silver nanowires for fabricating ultra-stretchable microtextiles with weakly and tunable negative permittivity, *Composites Science and Technology*, 2022, **223**, 109415, doi: 10.1016/j.compscitech.2022.109415.
[46] Yunpeng, Qu, Ultraweakly and fine-tunable negative permittivity of polyaniline/nickel metacomposites with high-frequency diamagnetic response, *Composites Science and Technology*, 2022, **217**, 109092, doi: 10.1016/j.compscitech.2021.109092.
[47] Guohua, Fan, Dielectric properties and negative permittivity performance modulated by dual fillers in CNTs/TiN/$CaCu_3Ti_4O_{12}$ ternary composites, *Ceramics International*, 2022, **48**, 28135-28141, doi: 10.1016/j.ceramint.2022.06.118.
[48] Y. Qu, J. Wu, Z. Wang, Y. Liu, P. Xie, Z. Wang, J. Tian, R. Fan, Radio-frequency epsilon-negative property and diamagnetic response of percolative Ag/CCTO metacomposites, *Scripta Materialia*, 2021, **203**, 114067, doi: 10.1016/j.scriptamat.2021.114067.
[49] Z.-C. Shi, R.-H. Fan, Z.-D. Zhang, L. Qian, M. Gao, M. Zhang, L.-T. Zheng, X.-H. Zhang, L.-W. Yin, Random composites of nickel networks supported by porous alumina toward double negative materials, *Advanced Materials*, 2012, **24**, 2349-2352, doi: 10.1002/adma.201200157.
[50] X. Wu, K. Liu, J. Ding, B. Zheng, F. Gao, K. Qian, Y. Ma, Y. Feng, L. Chen, P. Zhang, H. Wang, Construction of Ni-based alloys decorated sucrose-derived carbon hybrid towards: effective microwave absorption application, *Advanced Composites and Hybrid Materials*, 2022, **5**, 2260-2270, doi: 10.1007/s42114-021-00383-1.
[51] Z. Qu, J. Hao, H. Jing, Y. Wei, J. Duan, J. Wang, B. Zhang, An ultra-thin ultra-broadband microwave absorber for radar stealth, *Advanced Composites and Hybrid Materials*, 2022, **5**, 1778-1785, doi: 10.1007/s42114-022-00429-y.
[52] F. Luo, D. Liu, T. Cao, H. Cheng, J. Kuang, Y. Deng, W. Xie, Study on broadband microwave absorbing performance of gradient porous structure, *Advanced Composites and Hybrid Materials*, 2021, **4**, 591-601, doi: 10.1007/s42114-021-00275-4.
[53] Kai, Sun, Microwave absorption performance of magnetic-dielectric Fe_3O_4@C@PPy composites with a core-double-shell structure prepared by a low-temperature self-propagation method, *Ceramics International*, 2023, **49**, 35782-35791, doi: 10.1016/j.ceramint.2023.08.257.
[54] Z. Wang, K. Sun, P. Xie, Q. Hou, Y. Liu, Q. Gu, R. Fan, Design and analysis of negative permittivity behaviors in Barium titanate/nickel metacomposites, *Acta Materialia*, 2020, **185**, 412-419, doi: 10.1016/j.actamat.2019.12.034.
[55] K. Sun, X. Yang, Y. Lei, H. Du, T. Dudziak, R. Fan, Core-shell structural design and microwave absorption enhancement of multi-dimensional graphene oxide@polypyrrole/carbonyl iron fiber nanocomposites, *Journal of Alloys and Compounds*, 2023, **930**, 167446, doi: 10.1016/j.jallcom.2022.167446.
[56] S. Xia, Z. Shi, K. Sun, P. Yin, D. Dastan, Y. Liu, H. Cui, R. Fan, Achieving remarkable energy storage enhancement in polymer dielectrics *via* constructing an ultrathin Coulomb blockade layer of gold nanoparticles, *Materials Horizons*, 2023, **10**, 2476-2486, doi: 10.1039/d3mh00084b.
[57] Z.-C. Shi, R.-H. Fan, K.-L. Yan, K. Sun, M. Zhang, C.-G. Wang, X.-F. Liu, X.-H. Zhang, Preparation of iron networks hosted in porous alumina with tunable negative permittivity and permeability, *Advanced Functional Materials*, 2013, **23**, 4123-4132, doi: 10.1002/adfm.201202895.
[58] Y. Qu, Y. Du, G. Fan, J. Xin, Y. Liu, P. Xie, S. You, Z. Zhang, K. Sun, R. Fan, Low-temperature sintering graphene/$CaCu_3Ti_4O_{12}$ nanocomposites with tunable negative permittivity, *Journal of Alloys and Compounds*, 2019, **771**, 699-710, doi: 10.1016/j.jallcom.2018.09.049.
[59] Y.-P. Qu, H.-K. Wu, P.-T. Xie, N. Zeng, Y.-L. Chen, X. Gong, J.-L. Yang, Q. Peng, Y. Xie, X.-S. Qi, Carbon nanotube-carbon black/$CaCu_3Ti_4O_{12}$ ternary metacomposites with tunable negative permittivity and thermal conductivity fabricated by spark plasma sintering, *Rare Metals*, 2023, 1-11, doi: 10.1007/s12598-023-02346-5.
[60] Chunyuan, Deng, Highly tunable ε'-negative and ε'-near-zero response at extremely low frequency region of $CaCu_3Ti_4O_{12}$/graphitized-MWCNT metacomposites, *Composites Communications*, 2023, **43**, 101724, doi: 10.1016/j.coco.2023.101724.
[61] Y. Qu, P. Xie, Y. Zhou, J. Ding, Y. Chen, X. Gong, J. Yang, Q. Peng, X. Qi, Graphitized-MWCNT/$CaCu_3Ti_4O_{12}$ metacomposites for tunable ε'-negative and ε'-near-zero response with enhanced electromagnetic shielding, *Ceramics International*, 2023, **49**, 37407-37414, doi: 10.1016/j.ceramint.2023.09.066.
[62] Y. Qu, Q. Peng, Y. Zhou, F. Manshaii, S. Wang, K. Wang, P. Xie, X. Qi, K. Sun, Fine-tunable ε'-negative response derived from low-frequency plasma oscillation in graphene/polyaniline metacomposites, *Composites Communications*, 2023, **44**, 101750, doi: 10.1016/j.coco.2023.101750.

